

ORIGINAL RESEARCH

Biomarkers of immunogenic stress in metastases from melanoma patients: Correlations with the immune infiltrate

Sylvain Ladoire^{a,b,c,*}, Laura Senovilla^{d,e,f,g,*}, David Enot^{h,*}, François Ghiringhelli^{a,b}, Vichnou Poirier-Colame^c, Kariman Chaba^{d,e,f}, Gulsun Erdag^{ij}, Jochen T. Schaefer^{ij}, Donna H. Deacon^j, Laurence Zitvogel^{c,g,k}, Craig L. Slingluff Jr.^{j,#}, and Guido Kroemer^{d,e,f,h,l,m,#}

^aDepartment of Medical Oncology, Georges François Leclerc Center, Dijon, France; ^bInstitut National de la Santé et de la Recherche Médicale, Avenir Team INSERM, University of Burgundy, Dijon, France; ^cInstitut National de la Santé et de la Recherche Médicale, U1015, Equipe labellisée Ligue Nationale Contre le Cancer, Institut Gustave Roussy, Villejuif, France; ^dEquipe 11 labellisée par la Ligue Nationale contre le Cancer, Centre de Recherche des Cordeliers, Paris, France; ^eINSERM, U1138, Paris, France; ^fUniversité Paris Descartes, Sorbonne Paris Cité, Paris, France; ^gUniversity of Paris Sud XI, Villejuif, France; ^hMetabolomics and Cell Biology Platforms, Gustave Roussy Cancer Campus, Villejuif, France; ⁱDepartment of Pathology, University of Virginia, Charlottesville, VA, USA; ^jDepartment of Surgery, University of Virginia, Charlottesville, VA, USA; ^kCenter of Clinical Investigations in Biotherapies of Cancer (CICBT), Villejuif, France; ^lPôle de Biologie, Hôpital Européen Georges Pompidou, Assistance Publique-Hôpitaux de Paris, Paris, France; ^mKarolinska Institute, Department of Women's and Children's Health, Karolinska University Hospital, Stockholm, Sweden

ABSTRACT

Melanoma is known to be under latent immunosurveillance. Here, we studied four biomarkers of immunogenic cell stress and death (microtubule-associated proteins 1A/1B light chain 3B (MAP-LC3B, best known as LC3B)-positive puncta in the cytoplasm as a sign of autophagy; presence of nuclear HMGB1; phosphorylation of eIF2 α ; increase in ploidy) in melanoma cells, in tissue microarrays (TMA) from metastases from 147 melanoma patients. These biomarkers of immunogenicity were correlated with the density of immune cells infiltrating the metastases and expressing CD3, CD4⁺, CD8⁺, CD20, CD45, CD56, CD138, CD163, DC-LAMP or FOXP3. LC3B puncta positively correlated with the infiltration of metastases by CD163⁺ macrophages, while expression of HMGB1 correlated with infiltration by FOXP3⁺ regulatory T cells and CD56⁺ lymphocytes. eIF2 α phosphorylation was associated with an augmentation of nuclear diameters, reflecting an increase in ploidy. Interestingly, therapeutic vaccination led to a reduction of eIF2 α phosphorylation suggestive of immunoselection against cells bearing this sign of endoplasmic reticulum (ER) stress. None of the stress/death-related biomarkers had a significant prognostic impact, contrasting with the major prognostic effect of the ratio of cytotoxic T lymphocytes (CTL) over immunosuppressive FOXP3⁺ and CD163⁺ cells. Altogether, these results support the idea of a mutual dialog between, on one hand, melanoma cells with their cell-intrinsic stress pathways and, on the other hand, immune effectors. Future work is required to understand the detailed mechanisms of this interaction.

ARTICLE HISTORY

Received 8 February 2016
Revised 24 February 2016
Accepted 25 February 2016

KEYWORDS

Autophagy; HMGB1; immune infiltrates; immunogenic cell death; LC3; melanoma


Introduction

There is growing awareness that cancer including melanoma is not just a cell-autonomous disease and that malignancy only can develop in the context of failing immunosurveillance.¹⁻⁴ At least for melanoma, this concept has been fully proven at the clinical level, as demonstrated by the spectacular therapeutic success of immune checkpoint blockers neutralizing CTLA-4 or the PD-1/PD-L1 interaction.⁵⁻⁸ Indeed, even advanced, metastatic melanoma responds in most cases to the combined blockade of CTLA-4 and PD-1.⁹

One particular mechanism to induce an anticancer immune response is the induction of immunogenic cell death (ICD), a modality of cell death that is preceded by stress responses that alert the innate immune response.^{10,11} ICD is accompanied by the induction of autophagy, which facilitates the optimal release

of ATP by lysosomal exocytosis during the blebbing phase of apoptosis.^{12,13} Extracellular ATP is a potent chemotactic signal for inducing the infiltration of tumors by myeloid cells including dendritic cell (DC) precursors.^{12,14, 15} ICD is also preceded by ER stress leading to the phosphorylation of eukaryotic initiation factor 2 α (eIF2 α) and the subsequent exposure of calreticulin (CALR) at the surface of the cancer cell.^{16,17} Surface CALR then serves as an "eat-me" signal to facilitate the transfer of portions of the cancer cell into immature DCs, for subsequent cross-presentation of tumor antigens.¹⁸ After plasma membrane permeabilization, dead cells release high mobility group B1 (HMGB1) from their nuclei. HMGB1 then acts on toll-like receptor 4 (TLR4) on the surface of DCs to stimulate tumor antigen presentation.^{19,20}

CONTACT Guido Kroemer  Kroemer@orange.fr

 Supplemental data for this article can be accessed on the publisher's website.

*Shared co-first authorship.

#Shared senior authorship.

© 2016 Taylor & Francis Group, LLC

There is growing evidence that the aforementioned molecules and processes determine the anticancer immune response in patients with malignant diseases.^{21,22} Hence, disabled autophagy with primary cancer cells indicates poor prognosis in breast cancer,²³ correlating with signs of a poor local immune response and hence a reduced infiltration by CD8⁺ CTL and an enhanced infiltration by immunosuppressive FOXP3⁺ regulatory T cells or CD68⁺ macrophages, resulting in a major decline in CD8⁺/FOXP⁺ and CD8⁺/CD68⁺ ratios.²⁴ The suppression of autophagy can be deduced from the absence of LC3B puncta in the cytoplasm of malignant cells, as detectable by immunohistochemistry.^{23,25} Reduced expression of CALR by cancer cells has been correlated with poor prognosis and reduced infiltration by CTL in colorectal cancer,²⁶ as well as in non-small cell lung cancer (NSCLC).^{27,28} Similarly, low phosphorylation of eIF2 α , which can be measured by immunohistochemistry using a phospho-neoepitope-specific antibody, predicts poor local immune responses and dismal prognosis in NSCLC.²⁸ In breast cancer, eIF2 α phosphorylation could be associated with an increased ploidy (which induces ER stress and correlates with an increase in nuclear size) and the CD8⁺/FOXP⁺ ratio within tumor infiltrating T lymphocytes.²⁹ Absent HMGB1 expression correlated with a general drop in all immune effectors in breast cancers and indicated poor prognosis.^{23,24}

The aforementioned examples illustrate the tight relationship between immunogenic stress signals within cancer cells, the composition of the immune infiltrate and the evolution of malignant disease in several major carcinomas, namely, breast, lung and colorectal cancers. Based on this premise, we decided to investigate the impact of ICD-related biomarkers detectable by immunohistochemistry on a series of melanoma metastases that have previously been characterized for the composition of their immune infiltrate, confirming the contention that even late-stage melanoma is under immunosurveillance.³⁰ Our results reveal that ICD-related biomarkers within melanoma cells do affect the composition of the immune infiltrate of metastatic lesions. However, the impact of such ICD-related biomarkers on the immune infiltrate in melanoma metastases is quite different from that observed in primary lesions from major carcinomas.

Results and discussion

Prognostic impact of the immune infiltrate in melanoma metastases

As previously reported,³⁰ there is a strong positive correlation among the presence of distinct leukocyte populations in melanoma metastases. This applies to the density of cells bearing lymphocyte markers (CD20 expressed on B cells; CD138 expressed by plasma cells; CD3, CD4⁺ and CD8⁺ expressed on T cells; CD56 expressed on NK cells), DC markers (DC-LAMP) and even markers that have been linked to immunosuppression (CD163, FOXP3 and PD1, which are expressed by macrophages, regulatory T cells and exhausted lymphocytes, respectively) (Fig. S1). Accordingly, all but one of the infiltrating immune cell types tended to have a positive prognostic impact (which was significant, after adjustment for the clinical

stage, for cells expressing CD128, CD20, CD3, CD4⁺, CD8⁺, CD56 or FOXP3) on patient survival. Only CD163⁺ macrophages tended to have a – however non-significant – negative impact on patient survival (Fig. 1A). It may appear counterintuitive that the presence of immunosuppressive FOXP3⁺ T cells has a positive impact on patient survival. This paradox may be explained by the fact that the expression of immune cell subtypes tend to correlate among each other in a positive way (Fig. S1), meaning that even the presence of immunosuppressive subpopulations indicates the occurrence of an organized immune infiltrate.³¹ Accordingly, when calculating the ratios of the immune effectors with respect to FOXP3⁺ Tregs, a favorable frequency of CD20⁺/FOXP3⁺ and CD8⁺/FOXP3⁺ cells correlated with overall survival (OS). Similarly, the ratios of CD20⁺/CD163⁺ and CD8⁺/CD163⁺ cells had a positive impact on patient survival (Figs. 1A–E).

Immunohistochemical detection of stress-related biomarkers in melanoma metastases

We used established immunohistochemical methods^{23,25,29,32} for staining melanoma tissues for the detection of eIF2 α phosphorylation (a marker of ER stress), nuclear diameter (which correlates with ploidy), cytoplasmic LC3B puncta (a marker of autophagy) and nuclear HMGB1 (an endogenous ligand of TLR4). Quantitation focused on malignant (rather than stromal) cells and was based on intensity (for phospho-eIF2 α), diameter (for nuclei) or percentages of cells positive for cytoplasmic LC3B puncta or nuclear HMGB1 (Figs. 2A–H). As expected,²⁹ the intensity of eIF2 α phosphorylation positively correlated with nuclear size (Fig. 3A). In contrast, LC3B puncta and nuclear HMGB1 did not correlate among each other, nor did they correlate with eIF2 α phosphorylation and nuclear size (Figs. 3B–F). Hence, ER stress apparently does not impact on the autophagy-related LC3B puncta. Irrespective of these considerations, it appears that melanoma cells are heterogeneous with respect to stress markers. In the next step, we explored the relationship of such biomarkers to immune parameters.

Relationship between the immune infiltrate and eIF2 α phosphorylation or hyperploidy

eIF2 α phosphorylation and nuclear size both failed to correlate with any of the immune markers studied here, as exemplified by the absence of correlations between phospho-eIF2 α or nuclear diameter and the infiltration by CD8⁺/FOXP3⁺ or CD8⁺/CD163⁺ cells (Figs. 4A–D). Accordingly, in the whole cohort, phospho-eIF2 α or nuclear diameter had no significant impact (after adjustment) on overall patient survival (Figs. S2–5). Nonetheless melanomas with increased nuclear size (which may indicate pleomorphy) tended to have a worse prognosis with an adjusted *p*-value of 0.0527 (Fig. S4F). Interestingly, the level of eIF2 α phosphorylation declined among those patients that had been vaccinated before surgical removal of the tumor (Fig. 4E), suggesting that this life-extending measure³⁰ causes the elimination of particularly immunogenic cells with hyperphosphorylated eIF2 α . Nonetheless, we did not observe a similar reduction in nuclear

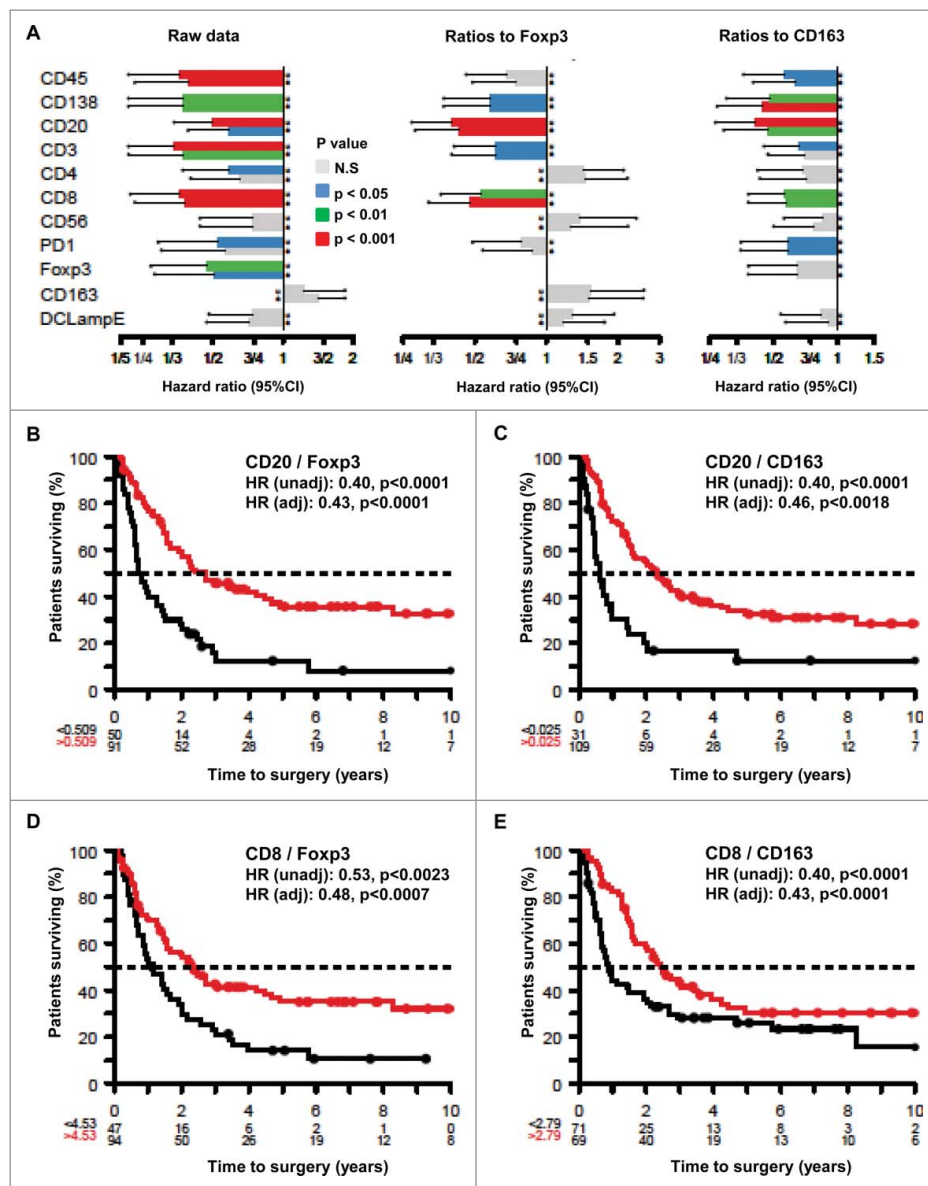


Figure 1. Prognostic impact of individual immune parameters and ratios between effector and suppressor cells measured by immunohistochemistry in melanoma metastases. (A) Impact of immune parameters on hazard ratios. The hazard ratios were calculated in an unadjusted (u) or adjusted (a) fashion for each of the indicated individual immune parameters or for the indicated ratios (each time after having calculated optimal cut-offs using log-rank statistics). Results are plotted together with the 95% confidence intervals. (B–E) Kaplan Meyer survival plots exemplifying the effects of distinct ratios between effector and suppressor cells on overall patient survival. Hazard ratios (HR) are indicated as unadjusted or adjusted values.

diameter (Fig. S5), suggesting that vaccination can affect eIF2 α phosphorylation without a concomitant effect on ploidy.

Immunological effects of LC3B puncta and HMGB1 expression

Significant ($p < 0.05$) positive correlations were observed between the presence of LC3B puncta in the cytoplasm of malignant cells and FOXP3⁺ or CD163⁺ immune infiltrates but not on other immune subtypes (Figs. 5A–C). Accordingly, a strong negative correlation was found when the percentage of malignant LC3B dot⁺ cells was plotted against the CD8⁺/FOXP3⁺ or CD8⁺/CD163⁺ ratios (Figs. 5D, E). We also observed a positive correlation between FOXP3⁺ (but not CD163⁺) infiltration and HMGB1 expression (Figs. 6A–C), reflecting a negative correlation between HMGB1 expression

and the CD8⁺/FOXP3⁺ (but not the CD8⁺/CD163⁺) ratio (Figs. 6D, E). However, no significant correlation between patient survival and LC3B puncta or HMGB1 expression could be detected (Figs. S6–9).

Concluding remarks

Previously, we have studied the relationship between prognosis, immune infiltrate and stress-associated biomarkers in breast and lung cancer. There are two striking differences between our prior work (on primary breast and lung cancer samples) and the present study (on melanoma metastases), although all these cancer types appear to be under strong immunosurveillance, meaning that the presence of an immune infiltrate and, more so, favorable ratios between immune effectors and immunosuppressive cell types predict improved

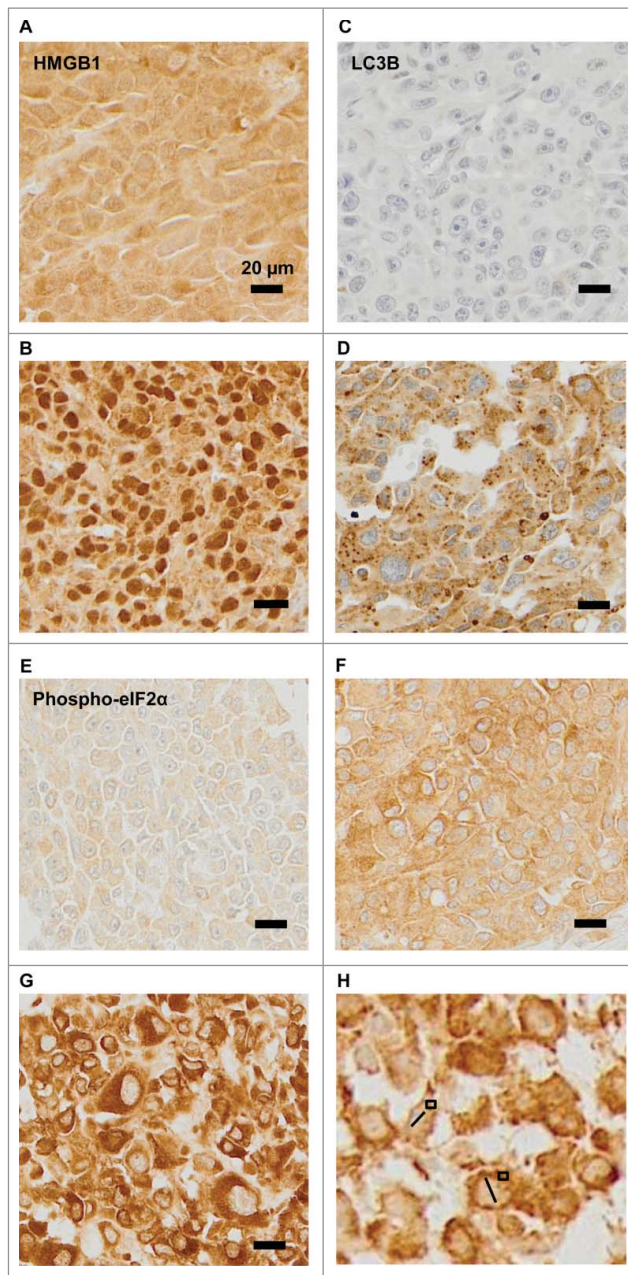


Figure 2. Representative immunohistochemical staining patterns. (A–B) Representative images of melanomas that are heterogeneous with respect to the presence of HMGB1 within nuclei (absence: A, presence: B). (C–D) Representative images of melanomas differing in the percentage of cells positive for cytoplasmic LC3B puncta (absence: C, presence D). (E–H) Representative images of phospho-eIF2 α -staining in melanoma metastases: (E): mild, (F): moderate, and (G): intense, (H): measures of nuclear diameters (bars), and phospho-eIF2 α -staining intensity (squares).

OS.^{21,31,33–39,28} First, none of the malignant cell stress-related biomarkers had any impact on melanoma patient survival, contrasting with the observation that the presence of LC3B puncta and high expression of HMGB1 has a positive effect on the life expectancy of breast cancer patients.²³ This discrepancy might be related to the stage of patients (operable breast cancer vs. stage III/IV melanoma), intrinsic biological differences between neoplasias (perhaps related to the epithelial vs. neuroectodermal origin of these tumor types), or a rather distinct organization of the immunosurveillance system. In favor of this latter hypothesis, there is a major difference between

breast cancer and melanoma. In primary breast cancers, the absence of LC3B puncta is accompanied by a major reduction in the CD8⁺/FOXP⁺ ratio (as well as the ratio of CD8⁺ T cells over CD68⁺ macrophages), contrasting with melanoma metastases in which scarce LC3B puncta correlate with an increase in the CD8⁺/FOXP⁺ ratio (as well as the ratio of CD8⁺ T cells over CD163⁺ macrophages). Similarly, in breast cancer, absent HMGB1 expression correlates with a general drop in all immune effectors, in particular FOXP3⁺ and CD68⁺ cells, contrasting with an increase of immune cells, in particular FOXP3⁺ and CD163⁺ cells, in melanoma metastases.

How can this paradox be resolved? As a possibility, in (early) breast cancer, immunosurveillance may be at a stage at which the potential release of DAMPs (ATP due to autophagy, HMGB1 due to its presence in nuclei) has a stimulatory effect on the anticancer immune response. In contrast, in (late) melanoma, immunosurveillance may be at a stage that is not any more depending on the release of DAMPs and at which malignant cells have been subjected to heavy immunoeediting (perhaps with the consequent elimination of cells that have the potential of DAMP release). The potential presence of such an immunoeediting process is indicated by the fact that tumors from patients that have undergone therapeutic vaccination exhibit reduced eIF2 α phosphorylation. However, such tumors do not exhibit any additional differences (with respect to nuclear size, LC3B puncta or HMGB1 expression), meaning that this explanation requires further validation.

In conclusion, the present study reveals unexpected links between cancer cell-intrinsic stress pathways and local immunosurveillance. Altogether, our findings support the idea of a strong reciprocal relationship between the tumor microenvironment and stress signals emitted by malignant cells.

Patients and methods

Patients

We reviewed surgical pathology reports of melanoma metastases in the Anatomic Pathology Software System (1982–2007), and 183 metastatic melanoma samples from 147 patients with clinical follow-up and ample surgical pathology material were selected to obtain core samples from at least three to four tumor regions to construct TMAs. The interval from date of surgery to date of last contact (death or last follow-up) ranged from 1 to 358 mo (mean: 37; median: 13.7 for deceased patients, 63 for alive patients). One-third of the patients (49) participated in experimental melanoma vaccine trials at Department of Surgery, University of Virginia, Charlottesville, nine of whom (18%) remained alive more than 5 y and were clinically free of disease at last follow-up. Of these, tumor was resected before, or after, enrolling in a vaccine trial.

Some patients had two to five synchronous or metachronous metastases. At surgery for the earliest specimen, 103 patients had stage III melanoma (4 IIIA, 40 IIIB, and 59 IIIC) and 44 had stage IV melanoma. Of the 183 specimens, 83 were in lymph nodes, 92 in skin and soft tissue, seven in small intestine, and one peritoneal. There were significant differences based on metastatic tissue site: melanomas metastatic to lymph nodes

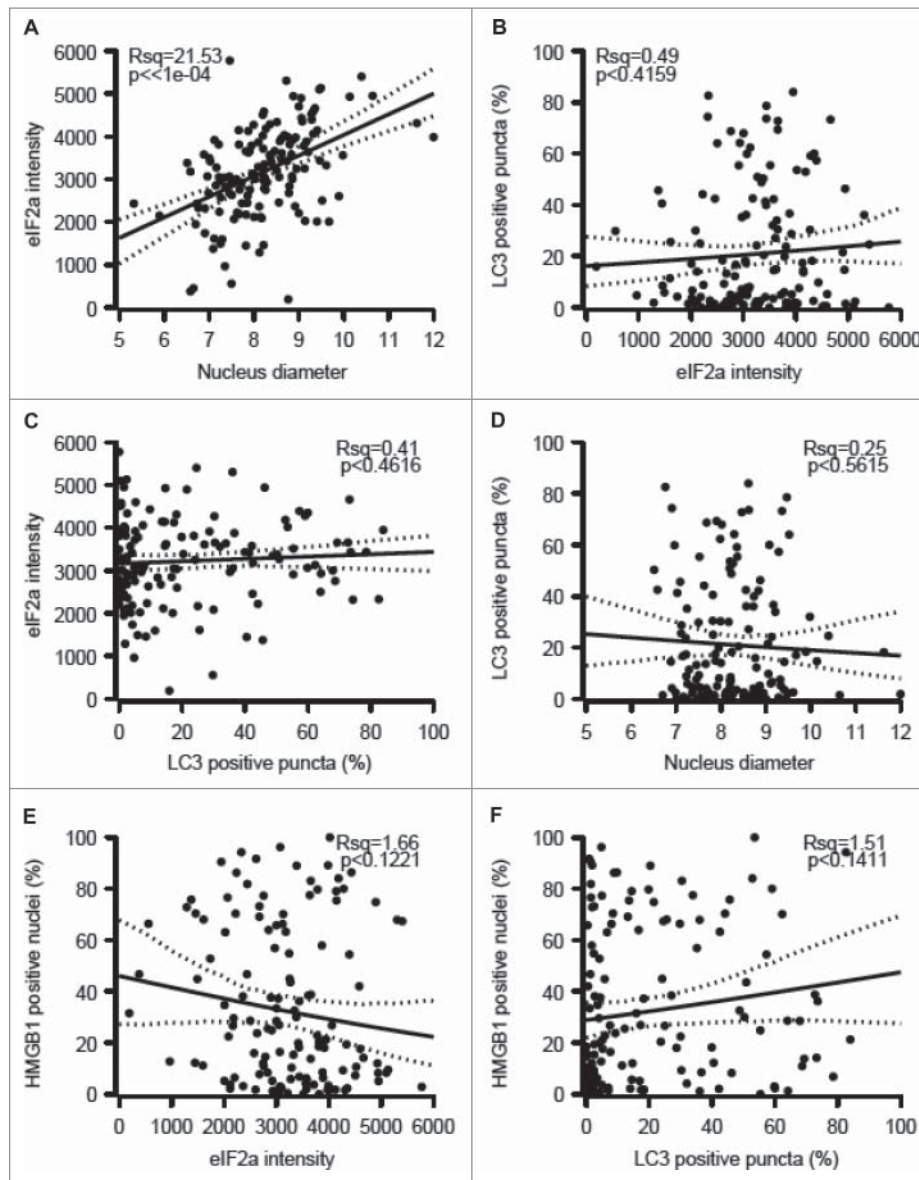


Figure 3. Correlations among melanoma cell-intrinsic biomarkers. The indicated parameters were quantified: eIF2 α as an intensity (A, C, E), nuclear diameter (B, D), LC3B as a frequency of cells exhibiting cytoplasmic puncta (C, E, F) and HMGB1 as a frequency of cells with positive nuclei (E, F) and the results were plotted against each other. psR²: pseudo r-squared.

contained higher numbers of CD45⁺, CD3⁺, CD8⁺, CD20⁺, and DC-LAMP⁺ cells compared with tumors metastatic to skin/soft tissue, small intestine, or peritoneum ($p < 0.001$, $p = 0.006$, $p = 0.019$, $p = 0.001$, and 0.035 , respectively). CD20⁺ B lymphocytes were highest in lymph nodes metastases and least prevalent in small bowel metastases. Macrophage (CD163) counts were similar among metastatic sites. CD56⁺ cell counts were very low in all groups, without significant differences.

Construction of tissue microarrays

Formalin-fixed paraffin-embedded (FFPE) tissue blocks were retrieved from archives of the Department of Pathology, University of Virginia. Use of human tissues was approved by the UVA Institutional Review Board (protocol 10598). Hematoxylin and eosin (H&E) slides from each block were reviewed by a pathologist (JS) to identify tumor areas. TMAs were constructed with 1.0-mm diameter tissue cores from representative

tumor areas from the FFPE tissue blocks, transferred into a recipient paraffin block using a semi-automated tissue array instrument (TMArrayer; Pathology Devices). Quadruplicate or triplicate tissue cores were taken from each specimen, resulting in nine composite TMA blocks containing tissue cores from 18 to 27 specimens each. Control tissues from spleen, liver, placenta, and kidney were included in each TMA block. Multiple 4- μ m sections were cut for H&E and immunohistochemical staining.

Immunohistochemistry for immune infiltrates

TMA tissue sections were deparaffinized in xylene and rehydrated by sequential incubation in ethanol/water solutions. Heat-induced antigen retrieval was performed in citrate buffer/low pH for most antibodies, or in EDTA/high pH buffer for antibodies directed to CD4⁺, CD8⁺, and CD56. Sections were incubated 60 min at room temperature (RT) with antibodies to

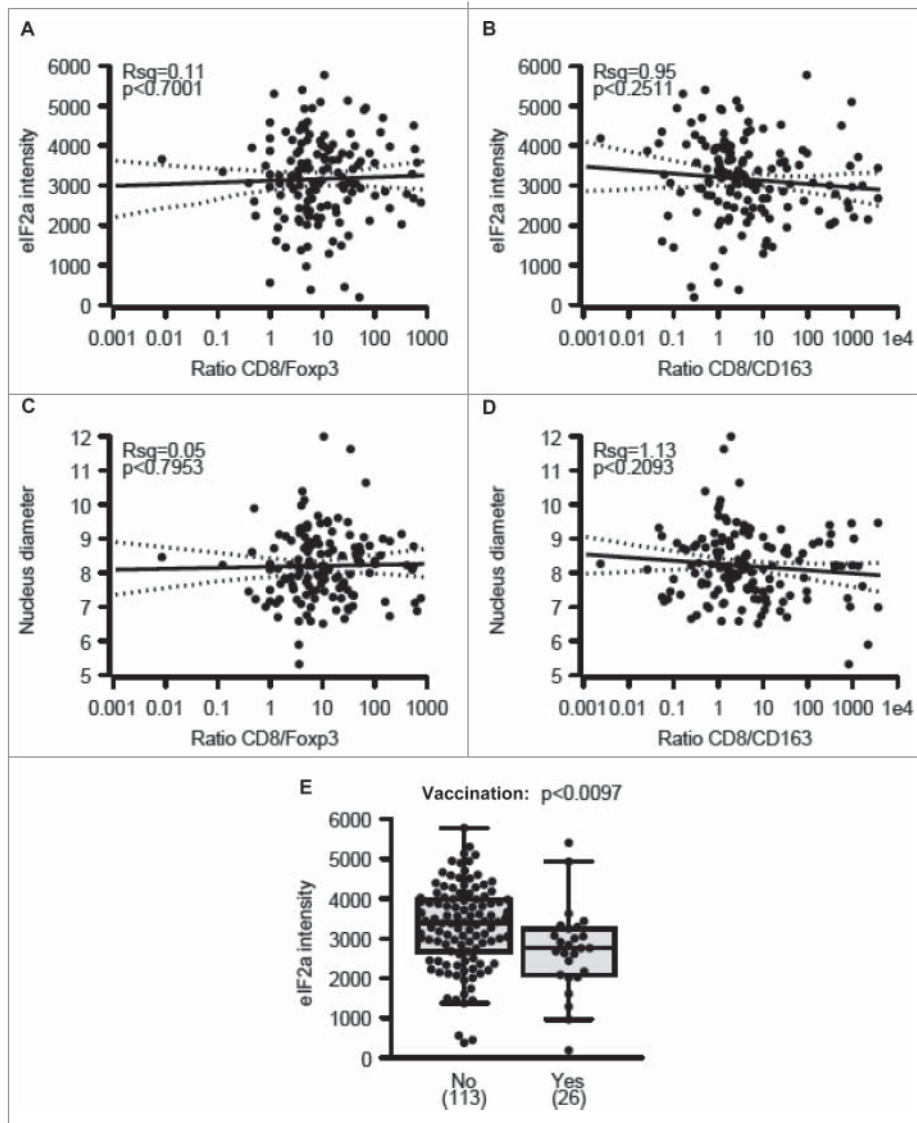


Figure 4. Correlations between eIF2 α phosphorylation, nuclear diameter, and immune parameters. (A–B) Correlations between phospho-eIF2 α intensity within malignant cells and the ratio of metastasis-infiltrating CD8 $^{+}$ over FOXP3 $^{+}$ (A) and CD163 $^{+}$ cells (B) (C–D) Correlations between nuclear diameters within melanoma cells and the ratio of metastasis-infiltrating CD8 $^{+}$ over FOXP3 $^{+}$ (C) and CD163 $^{+}$ cells (D). (E) Impact of therapeutic vaccination before resection of the primary tumor on the level of eIF2 α phosphorylation within melanoma metastases. Results in (E) are shown as box plots.

CD34 (1:100), CD45 (1:400), CD20 (1:400), CD3 (1:400), CD8 $^{+}$ (1:200), CD138 (1:100) from Dako, and to CD4 $^{+}$ (1:120; Vector Laboratories), CD56 (1:100; Invitrogen), CD163 (1:50; Santa Cruz Biotechnology Inc.), DC-LAMP (1:50; Dendritics), FoxP3 (1:125; EBioscience), and PD-1 (1:100; R&D Systems). Envision system (enzyme-conjugated polymer backbone coupled to secondary antibodies) and 3,30-diaminobenzidine chromogen (Dako) were applied to develop the staining. After rinsing with water, sections were counterstained with Hematoxylin (Vector Laboratories) and coverslipped with mounting medium (Vecta-Mount; Vector Laboratories).

Immunohistochemistry for biomarkers of immunogenic stress

HMGB1 staining: Formalin-fixed, paraffin-embedded TMA sections were deparaffinized with three successive passages through xylene, and rehydrated by sequential incubation in ethanol/water solutions. Antigen retrieval was carried out by

heating slides for 30 min in pH 6.0 citrate buffer at 98°C and cooling them for 45 min, at RT. The TMA sections were mounted on Shandon Sequenza coverplates (Thermo Fisher Scientific, 72-199-50) in distilled water. Sections were then saturated 20 min with Protein Block Serum Free (DAKO). Without washing, the primary antibody, a polyclonal rabbit anti HMGB1 antibody (4 μ g/mL, # PA1-16926, ThermoScientist Pierce), was incubated overnight. Endogenous peroxidase activity was inhibited with 3% hydrogen peroxidase (DAKO) for 15 min followed by the secondary antibody (Envision-Rabbit, Dako) for 45 min. Peroxidase activity was revealed by means of diaminobenzidine substrate (DAB, Dako), and the sections were counterstained with Mayer's hematoxylin.²⁰

LC3B staining: We previously described a validated immunohistochemical protocol for the detection of LC3B puncta in human FFPE cancer specimens.²⁵ Briefly, immunohistochemical staining of TMA sections was performed using the Novolink Kit (Menarini Diagnostics, RE7140-K). Deparaffinized and heated tissue sections for 30 min in pH 6.0 citrate buffer at

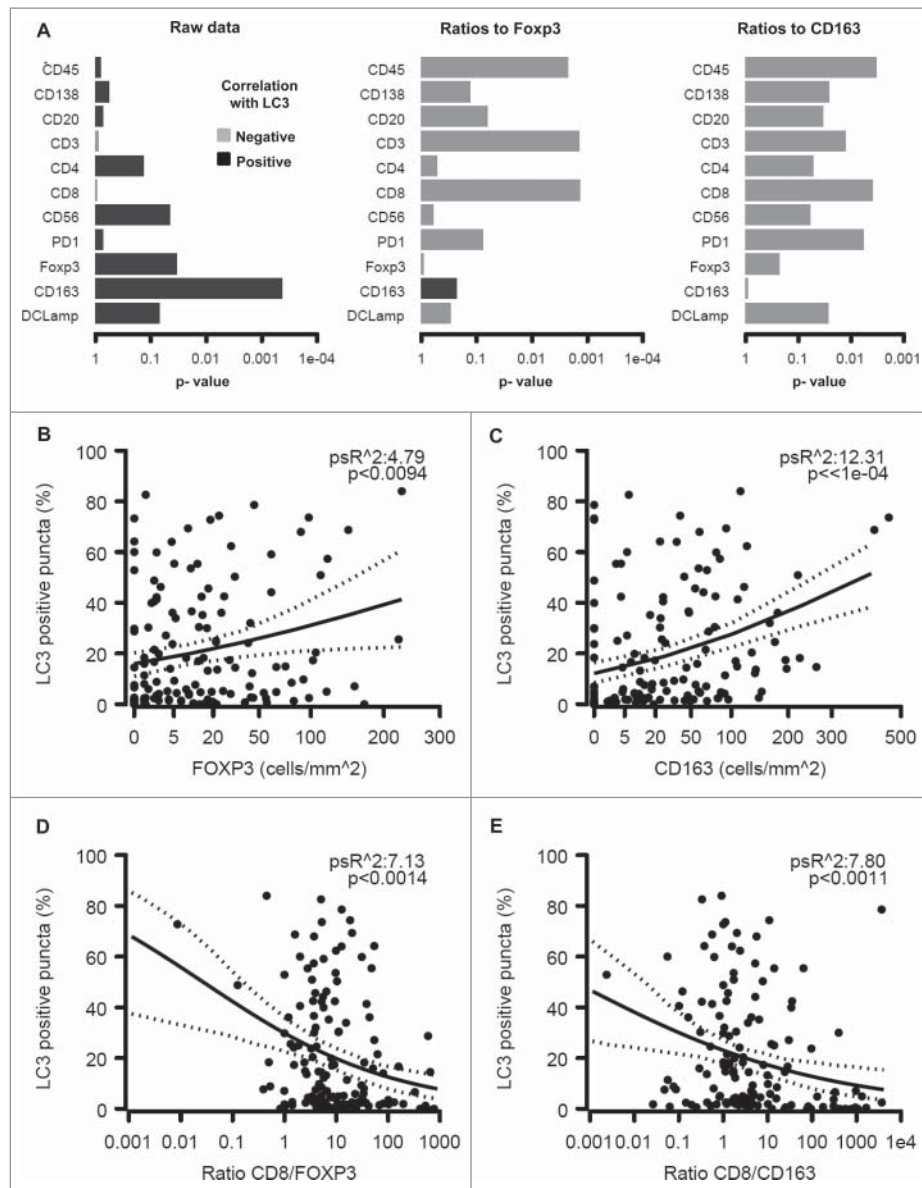


Figure 5. Relationship between LC3B puncta in melanoma cells and the immune infiltrate. The overall analysis of the correlation between LC3B puncta on individual immune parameters or the indicated ratios is shown (A). Also are shown the impact of LC3B puncta on the density of the infiltration by FOXP3⁺ T lymphocytes (B), CD163⁺ macrophages (C), the ratio of CD8⁺/FOXP3⁺ cells (D) and the ratio of CD8⁺/CD163⁺ cells (E).

95°C were allowed to cool down for 45 min, at RT and mounted on Shandon Sequenza coverplates (Thermo Fisher Scientific, 72-199-50) in distilled water, and then washed twice for 5 min with 0.1% Tween 20 (v/v in PBS). Thereafter, sections were incubated for 5 min with the Peroxidase Block reagent, and subsequently washed twice for 5 min with 0.1% Tween 20 (v/v in PBS). Following a 5 min long incubation at RT with the Protein Block reagent, tissue sections were washed twice for 5 min with 0.1% Tween 20 (v/v in PBS), and then incubated overnight at 4°C with a primary antibody specific for LC3B (clone 5F10, Nanotools, 0231-100), dissolved in 1% bovine serum albumin (w/v in TBS) at the final concentration of 25 µg/mL. This antibody recognizes both the soluble (LC3-I) and the membrane-bound form (LC3-II) of LC3B. After two washes in 0.1% Tween 20 (v/v in PBS), sections were incubated for 30 min with the Post Primary Block reagent, washed again as before and incubated for 30 min with secondary antibodies

coupled to horseradish peroxidase. Upon two additional washes, secondary antibodies were revealed with the liquid DAB Substrate Chromogen system (10 min). Finally, slides were washed in distilled water, and counterstained with hematoxylin.

Phospho-eIF2 α (phospho S51) staining

Formalin-fixed, paraffin-embedded TMA sections were deparaffinized with three successive passages through xylene, and rehydrated by sequential incubation in ethanol/water solutions. Antigen retrieval was carried out by heating slides for 20 min in pH 7.3 citrate buffer at 98°C and cooling them for 30 min, RT. The TMA sections were mounted on Shandon Sequenza coverplates (Thermo Fisher Scientific, 72-199-50) in distilled water. Sections were then saturated 2 h with TBS-1% BSA-10% of goat serum (VECTOR). Without washing, the primary antibody, a monoclonal rabbit anti Anti-Phospho-eIF2 α (phospho

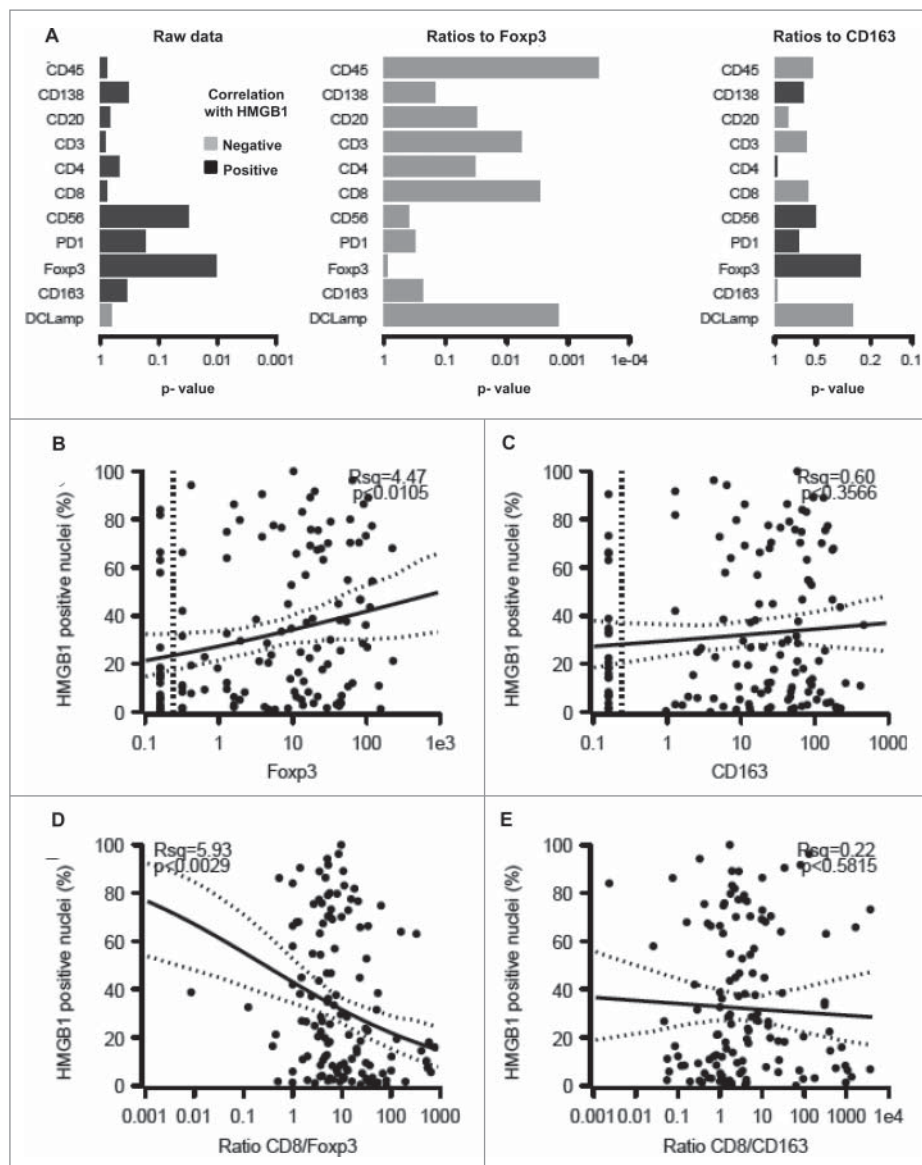


Figure 6. Correlation between HMGB1 expression by melanoma cells and the immune infiltrate. The overall correlation between HMGB1 expression and individual immune parameters or the calculated ratios is shown (A). Also are shown the impact of HMGB1 expression on the infiltration by FOXP3⁺ T lymphocytes (B), CD163⁺ macrophages (C), the ratio of CD8⁺/FOXP3⁺ cells (D) and the ratio of CD8⁺/CD163⁺ cells (E).

S51) antibody (7 μ g/mL, # ab32157, abcam), was incubated overnight. Endogenous peroxidase activity was inhibited with 3% hydrogen peroxidase (DAKO) for 15 min followed by the secondary antibody (Envision-Rabbit, Dako) for 45 min. Peroxidase activity was revealed by means of daminobenzidine substrate (DAB, Dako), and the sections were counterstained with Mayer's hematoxylin.

Pathologic assessment

Quantification of immune cells

Tumor-infiltrating immune cells were quantified on H&E-stained sections. Cores with no tumor tissue, more than 50% necrosis, or hemorrhage were excluded. Stained cells were enumerated by a pathologist (GE) on each core in a high-power microscope field, excluding cells within blood vessels or in hemorrhagic or necrotic areas. Cell counts were normalized to per mm². Images were obtained using an Olympus BX51

microscope coupled to an Olympus BP70 digital camera (Olympus America Inc.), and software Image ProPlus 4.5 for Windows.

Pathologic assessment for biomarkers of immunogenic stress

For HMGB1 staining, the pattern of expression (nuclear or not) was evaluated in tumor cells: strong nuclear staining of at least 50% of the tumor cells was considered positive for HMGB1 tumor expression. The presence of LC3B puncta in tumor cells and the percentage of tumor cells with detectable LC3B puncta were assessed, independently of the intensity of diffuse cytoplasmic staining. Considering the possibility of tumor heterogeneity, LC3B pathological evaluations were done on the whole tumor area and at least 15 high-power fields (x20).

Concerning phospho-eIF2 α , after staining, images were acquired with a virtual slide microscope VS120-SL (Olympus, Tokyo, Japan), 20x air objective (0.75 NA). VSI coded images

were transformed into TIFF file format using the OliVIA image viewer software. These images were thereafter analyzed by the public program ImageJ. Nuclear diameter was obtained measuring the straight tool. Phospho-eIF2 α quantification was carried out calculating the integrated density of a predetermined rectangular selection on representative stained cells.

Statistical analysis

Clinicopathological characteristics were available for 143 patients (see Table S1). Data analyses and representations were performed within the statistical environment R. Individual data points representing the measurement from one patient were systematically graphed alongside with the box-and-whisker plots calculated from the corresponding distribution. Proportions of positive HMGB1 and LC3 spots were modeled by quasi-binomial logistic regression from the overall count of spots, whereas eIF2 α averaged intensity, averaged nucleus diameter, immunological parameters (after square root transformation), and ratios between them (after log transformation) were modeled by linear regression. Spearman rho statistics, Kruskal Wallis and Wilcoxon rank-sum tests were also presented for comparison.

OS was determined from the date of surgery and censored at the last follow-up date (missing for one patient) or at 10 y (eight patients). Survival curves were estimated by the Kaplan-Meier product-limit method and their distributions compared by Cox proportional hazards regression. Multivariate adjustment was performed on patient age at surgery and disease stage (IIIA+B vs. IIIC vs. IV) and. Unless stated otherwise, *p*-values are two-sided, reported together with the back-transformed 95% confidence intervals for the statistics of interest and considered significant when <0.05 . To determine adequate cutoff values for patient survival stratification, the martingale residuals for the MFS Cox regression model, and log-rank statistics of all possible cutpoints were calculated.⁴⁰

Disclosure of potential conflicts of interest

No potential conflicts of interest were disclosed.

Funding

GK and LZ are supported by the Ligue contre le Cancer (équipes labélisées); Agence Nationale de la Recherche (ANR); Association pour la recherche sur le cancer (ARC); Cancéropôle Ile-de-France; Institut National du Cancer (INCa); Fondation Bettencourt-Schueller; Fondation de France; Fondation pour la Recherche Médicale (FRM); the European Commission (ArtForce); the European Research Council (ERC for GK); the LabEx Immuno-Oncology; the SIRIC Stratified Oncology Cell DNA Repair and Tumor Immune Elimination (SOCRATE); the SIRIC Cancer Research and Personalized Medicine (CARPEM); and the Paris Alliance of Cancer Research Institutes (PACRI). LZ was supported by ISREC and Swiss Bridge Foundation.

References

- Kroemer G, Pouyssegur J. Tumor cell metabolism: cancer's Achilles' heel. *Cancer Cell* 2008; 13:472-82; PMID:18538731; <http://dx.doi.org/10.1016/j.ccr.2008.05.005>
- Hanahan D, Weinberg RA. Hallmarks of cancer: the next generation. *Cell* 2011; 144:646-74; PMID:21376230; <http://dx.doi.org/10.1016/j.cell.2011.02.013>
- Schreiber RD, Old LJ, Smyth MJ. Cancer immunoediting: integrating immunity's roles in cancer suppression and promotion. *Science* 2011; 331:1565-70; PMID:21436444; <http://dx.doi.org/10.1126/science.1203486>
- Zitvogel L, Galluzzi L, Smyth MJ, Kroemer G. Mechanism of action of conventional and targeted anticancer therapies: reinstating immunosurveillance. *Immunity* 2013; 39:74-88; PMID:23890065; <http://dx.doi.org/10.1016/j.immuni.2013.06.014>
- Allison JP. Checkpoints. *Cell* 2015; 162:1202-5; PMID:26359978; <http://dx.doi.org/10.1016/j.cell.2015.08.047>
- Chandra RA, Wilhite TJ, Balboni TA, Alexander BM, Spektor A, Ott PA, Ng AK, Hodi FS, Schoenfeld JD. A systematic evaluation of abscopal responses following radiotherapy in patients with metastatic melanoma treated with ipilimumab. *Oncoimmunology* 2015; 4:e1046028; PMID:26451318; <http://dx.doi.org/10.1080/2162402X.2015.1046028>
- Kroemer G, Galluzzi L. Combinatorial immunotherapy with checkpoint blockers solves the problem of metastatic melanoma—an exclamation sign with a question mark. *Oncoimmunology* 2015; 4:e1058037; PMID:26140249; <http://dx.doi.org/10.1080/2162402X.2015.1058037>
- Galluzzi L, Kroemer G, Eggermont A. Novel immune checkpoint blocker approved for the treatment of advanced melanoma. *Oncoimmunology* 2014; 3:e967147; PMID:25941597; <http://dx.doi.org/10.4161/21624011.2014.967147>
- Larkin J, Chiarion-Sileni V, Gonzalez R, Grob JJ, Cowey CL, Lao CD, Schadendorf D, Dummer R, Smylie M, Rutkowski P et al. Combined Nivolumab and Ipilimumab or monotherapy in untreated melanoma. *N Engl J Med* 2015; 373:23-34; PMID:26027431; <http://dx.doi.org/10.1056/NEJMoa1504030>
- Kroemer G, Galluzzi L, Kepp O, Zitvogel L. Immunogenic cell death in cancer therapy. *Annu Rev Immunol* 2013; 31:51-72; PMID:23157435; <http://dx.doi.org/10.1146/annurev-immunol-032712-100008>
- Kepp O, Senovilla L, Vitale I, Vacchelli E, Adjemian S, Agostinis P, Apetoh L, Aranda F, Barnaba V, Bloy N et al. Consensus guidelines for the detection of immunogenic cell death. *Oncoimmunology* 2014; 3:e955691; PMID:25941621; <http://dx.doi.org/10.4161/21624011.2014.955691>
- Michaud M, Martins I, Sukkurwala AQ, Adjemian S, Ma Y, Pellegatti P, Shen S, Kepp O, Scoazec M, Mignot G et al. Autophagy-dependent anticancer immune responses induced by chemotherapeutic agents in mice. *Science* 2011; 334:1573-7; PMID:22174255; <http://dx.doi.org/10.1126/science.1208347>
- Martins I, Wang Y, Michaud M, Ma Y, Sukkurwala AQ, Shen S, Kepp O, Metivier D, Galluzzi L, Perfettini JL et al. Molecular mechanisms of ATP secretion during immunogenic cell death. *Cell Death Differ* 2014; 21:79-91; PMID:23852373; <http://dx.doi.org/10.1038/cdd.2013.75>
- Ma Y, Adjemian S, Mattarollo SR, Yamazaki T, Aymeric L, Yang H, Portela Catani JP, Hannani D, Duret H, Steegh K et al. Anticancer chemotherapy-induced intratumoral recruitment and differentiation of antigen-presenting cells. *Immunity* 2013; 38:729-41; PMID:23562161; <http://dx.doi.org/10.1016/j.immuni.2013.03.003>
- Ma Y, Galluzzi L, Zitvogel L, Kroemer G. Autophagy and cellular immune responses. *Immunity* 2013; 39:211-27; PMID:23973220; <http://dx.doi.org/10.1016/j.immuni.2013.07.017>
- Obeid M, Tesniere A, Ghiringhelli F, Fimia GM, Apetoh L, Perfettini JL, Castedo M, Mignot G, Panaretakis T, Casares N et al. Calreticulin exposure dictates the immunogenicity of cancer cell death. *Nat Med* 2007; 13:54-61; PMID:17187072; <http://dx.doi.org/10.1038/nm1523>
- Panaretakis T, Joza N, Modjtahedi N, Tesniere A, Vitale I, Durchschlag M, Fimia GM, Kepp O, Piacentini M, Froehlich KU et al. The co-translocation of ERp57 and calreticulin determines the immunogenicity of cell death. *Cell Death Differ* 2008; 15:1499-509; PMID:18464797; <http://dx.doi.org/10.1038/cdd.2008.67>
- Vacchelli E, Ma Y, Baracco EE, Sistigu A, Enot DP, Pietrocola F, Yang H, Adjemian S, Chaba K, Semeraro M et al. Chemotherapy-induced antitumor immunity requires formyl peptide receptor 1. *Science* 2015; 350(6263):972-8; PMID:26516201; <http://dx.doi.org/10.1126/science.aad0779>

19. Apetoh L, Ghiringhelli F, Tesniere A, Obeid M, Ortiz C, Criollo A, Mignot G, Maiuri MC, Ullrich E, Saulnier P et al. Toll-like receptor 4-dependent contribution of the immune system to anticancer chemotherapy and radiotherapy. *Nat Med* 2007; 13:1050-9; PMID:17704786; <http://dx.doi.org/10.1038/nm1622>
20. Yamazaki T, Hannani D, Poirier-Colame V, Ladoire S, Locher C, Sistigu A, Prada N, Adjemian S, Catani JP, Freudenberg M et al. Defective immunogenic cell death of HMGB1-deficient tumors: compensatory therapy with TLR4 agonists. *Cell Death Differ* 2014; 21:69-78; PMID:23811849; <http://dx.doi.org/10.1038/cdd.2013.72>
21. Kroemer G, Senovilla L, Galluzzi L, Andre F, Zitvogel L. Natural and therapy-induced immunosurveillance in breast cancer. *Nat Med* 2015; 21(10):1128-38; In Press; PMID:26444637; <http://dx.doi.org/10.1038/nm.3944>
22. Galluzzi L, Buque A, Kepp O, Zitvogel L, Kroemer G. Immunological effects of conventional chemotherapy and targeted anticancer agents. *Cancer Cell* 2015; 28(6):690-714; In press; PMID:26678337; <http://dx.doi.org/10.1016/j.ccell.2015.10.012>
23. Ladoire S, Penault-Llorca F, Senovilla L, Dalban C, Enot D, Locher C, Prada N, Poirier-Colame V, Chaba K, Arnould L et al. Combined evaluation of LC3B puncta and HMGB1 expression predicts residual risk of relapse after adjuvant chemotherapy in breast cancer. *Autophagy* 2015; 11(10):1878-90; In Press; PMID:26506894; <http://dx.doi.org/10.1080/15548627.2015.1082022>
24. Ladoire S, Enot D, Senovilla L, Ghiringhelli F, Poirier-Colame V, Chaba K, Semeraro M, Chaix M, Penault-Llorca F, Arnould L et al. The presence of LC3B puncta and HMGB1 expression in malignant cells correlate with the immune infiltrate in breast cancer. *Autophagy* 2016; 12(5):864-75; PMID:26979828; <http://dx.doi.org/10.1080/15548627.2016.1154244>
25. Ladoire S, Chaba K, Martins I, Sukkurwala AQ, Adjemian S, Michaud M, Poirier-Colame V, Andreiuolo F, Galluzzi L, White E et al. Immunohistochemical detection of cytoplasmic LC3 puncta in human cancer specimens. *Autophagy* 2012; 8:1175-84; PMID:22647537; <http://dx.doi.org/10.4161/auto.20353>
26. Peng RQ, Chen YB, Ding Y, Zhang R, Zhang X, Yu XJ, Zhou ZW, Zeng YX, Zhang XS. Expression of calreticulin is associated with infiltration of T-cells in stage IIIB colon cancer. *World J Gastroenterol* 2010; 16:2428-34; PMID:20480531; <http://dx.doi.org/10.3748/wjg.v16.i19.2428>
27. Fucikova J, Kralikova P, Fialova A, Brtnicky T, Rob L, Bartunkova J, Spisek R. Human tumor cells killed by anthracyclines induce a tumor-specific immune response. *Cancer Res* 2011; 71:4821-33; PMID:21602432; <http://dx.doi.org/10.1158/0008-5472.CAN-11-0950>
28. Fucikova J, Becht E, Iribarren K, Goc J, Remark R, Damotte D, Alifano M, Devi P, Biton J, Germain C et al. Calreticulin expression by non-small-cell lung cancer correlates with signs of immunosurveillance and favorable prognosis. *Cancer Res* 2016; In press; PMID:26842877
29. Senovilla L, Vitale I, Martins I, Tailler M, Pailleret C, Michaud M, Galluzzi L, Adjemian S, Kepp O, Niso-Santano M et al. An immunosurveillance mechanism controls cancer cell ploidy. *Science* 2012; 337:1678-84; PMID:23019653; <http://dx.doi.org/10.1126/science.1224922>
30. Erdag G, Schaefer JT, Smolkin ME, Deacon DH, Shea SM, Dengel LT, Patterson JW, Slingluff CL, Jr. Immunotype and immunohistologic characteristics of tumor-infiltrating immune cells are associated with clinical outcome in metastatic melanoma. *Cancer Res* 2012; 72:1070-80; PMID:22266112; <http://dx.doi.org/10.1158/0008-5472.CAN-11-3218>
31. Stoll G, Bindea G, Mlecnik B, Galon J, Zitvogel L, Kroemer G. Meta-analysis of organ-specific differences in the structure of the immune infiltrate in major malignancies. *Oncotarget* 2015; 6:11894-909; PMID:26059437; <http://dx.doi.org/10.18632/oncotarget.4180>
32. Bloy N, Sauvat A, Chaba K, Buque A, Humeau J, Bravo-San Pedro JM, Bui J, Kepp O, Kroemer G, Senovilla L. Morphometric analysis of immunoselection against hyperploid cancer cells. *Oncotarget* 2015; 6(38):41204-15; PMID:26517677; <http://dx.doi.org/10.18632/oncotarget.5400>
33. Denkert C, Loibl S, Noske A, Roller M, Muller BM, Komor M, Budczies J, Darb-Esfahani S, Kronenwett R, Hantusch C et al. Tumor-associated lymphocytes as an independent predictor of response to neoadjuvant chemotherapy in breast cancer. *J Clin Oncol* 2010; 28:105-13; PMID:19917869; <http://dx.doi.org/10.1200/JCO.2009.23.7370>
34. Stoll G, Enot D, Mlecnik B, Galon J, Zitvogel L, Kroemer G. Immune-related gene signatures predict the outcome of neoadjuvant chemotherapy. *Oncoimmunology* 2014; 3:e27884; PMID:24790795; <http://dx.doi.org/10.4161/onci.27884>
35. Stoll G, Zitvogel L, Kroemer G. Differences in the composition of the immune infiltrate in breast cancer, colorectal carcinoma, melanoma and non-small cell lung cancer: a microarray-based meta-analysis. *eCollection* 2016 Feb.5(2):e1067746; PMID: 27057431
36. Dieci MV, Criscitiello C, Goubar A, Viale G, Conte P, Guarneri V, Ficarra G, Mathieu MC, Delalogue S, Curigliano G et al. Prognostic value of tumor-infiltrating lymphocytes on residual disease after primary chemotherapy for triple-negative breast cancer: a retrospective multicenter study. *Ann Oncol* 2015; 26:1518; PMID:26109735; <http://dx.doi.org/10.1093/annonc/mdv239>
37. Dieci MV, Mathieu MC, Guarneri V, Conte P, Delalogue S, Andre F, Goubar A. Prognostic and predictive value of tumor-infiltrating lymphocytes in two phase III randomized adjuvant breast cancer trials. *Ann Oncol* 2015; 26:1698-704; PMID:25995301; <http://dx.doi.org/10.1093/annonc/mdv239>
38. Ladoire S, Arnould L, Apetoh L, Coudert B, Martin F, Chauffert B, Fumoleau P, Ghiringhelli F. Pathologic complete response to neoadjuvant chemotherapy of breast carcinoma is associated with the disappearance of tumor-infiltrating foxp3+ regulatory T cells. *Clin Cancer Res* 2008; 14:2413-20; PMID:18413832; <http://dx.doi.org/10.1158/1078-0432.CCR-07-4491>
39. Ladoire S, Mignot G, Dabakuyo S, Arnould L, Apetoh L, Rebe C, Coudert B, Martin F, Bizollon MH, Vanoli A et al. In situ immune response after neoadjuvant chemotherapy for breast cancer predicts survival. *J Pathol* 2011; 224:389-400; PMID:21437909; <http://dx.doi.org/10.1002/path.2866>
40. Hothorn T, Lausen B. On the exact distribution of maximally selected rank statistics. *Computational Statistics & Data Analysis* 2003; 43:121-37; [http://dx.doi.org/10.1016/S0167-9473\(02\)00225-6](http://dx.doi.org/10.1016/S0167-9473(02)00225-6)